China Geology 3 (2021) 476–486

China Geology

Journal homepage: http://chinageology.cgs.cn
https://www.sciencedirect.com/journal/china-geology

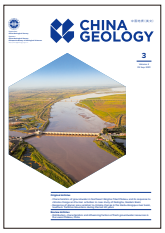

Hydrogeochemical characteristics of groundwater and pore-water and the paleoenvironmental evolution in the past 3.10 Ma in the Xiong'an New Area, North China

Kai Zhao[a, b], Jing-xian Qi[c], Yi Chen[d, e], Bai-heng Ma[a, f,*], Li Yi[a, f], Hua-ming Guo[e], Xin-zhou Wang[a, f], Lin-ying Wang[a, f], Hai-tao Li[b,*]

[a] *Hebei Key Laboratory of Geological Resources and Environment Monitoring and Protection*, *Shijiazhuang* 050021, *China*
[b] *China Institute of Geo-environmental monitoring*, *China Geological Survey*, *Beijing* 100081, *China*
[c] *Technical Centre for Soil, Agriculture and Rural Ecology and Environment*, *Ministry of Ecology and Environment*, *Beijing* 100012, *China*
[d] *Lianhe Equator Environmental Impact Assessment Co., Ltd.*, *Tianjin* 300042, *China*
[e] *China University of Geoscience (Beijing)*, *Beijing* 100083, *China*
[f] *Hebei Geological Environment Monitoring Institute*, *Shijiazhuang* 050021, *China*

ARTICLE INFO

Article history:
Received 3 August 2021
Received in revised form 7 September 2021
Accepted 14 September 2021
Available online 18 September 2021

Keywords:
Groundwater
Pore-water
Hydrogeochemistry
Stable oxygen isotope
Paleoclimate change
Paleoenvironmental reconstruction
Hydrogeological survey engineering
Xiong'an New Area
North China

ABSTRACT

The groundwater level has been continuously decreasing due to climate change and long-time overexploitation in the Xiong'an New Area, North China, which caused the enhanced mixing of groundwater in different aquifers and significant changes in regional groundwater chemistry characteristics. In this study, groundwater and sediment pore-water in drilling cores obtained from a 600 m borehole were investigated to evaluate hydrogeochemical processes in shallow and deep aquifers and paleo-environmental evolution in the past ca. 3.10 Ma. Results showed that there was no obvious change overall in chemical composition along the direction of groundwater runoff, but different hydrochemical processes occurred in shallow and deep groundwater in the vertical direction. Shallow groundwater (< 150 m) in the Xiong'an New Area was characterized by high salinity (TDS > 1000 mg/L) and high concentrations of Mn and Fe, while deep groundwater had better water quality with lower salinity. The high TDS values mostly occurred in aquifers with depth < 70 m and >500 m below land surface. Water isotopes showed that aquifer pore-water mostly originated from meteoric water under the influence of evaporation, and aquitard pore-water belonged to Paleo meteoric water. In addition, the evolution of the paleoclimate since 3.10 Ma BP was reconstructed, and four climate periods were determined by the $\delta^{18}O$ profiles of pore-water and sporopollen records from sediments at different depths. It can be inferred that the Quaternary Pleistocene (0.78–2.58 Ma BP) was dominated by the cold and dry climate of the glacial period, with three interglacial intervals of warm and humid climate. What's more, this study demonstrates the possibilities of the applications of pore-water on the hydrogeochemical study and further supports the finding that pore-water could retain the feature of paleo-sedimentary water.

1. Introduction

On April 1st, 2017, China's government statement reported the plan to set up Xiong'an New Area (also referred to as New Area), which aims to relieve Beijing of functions non-essential to its role as China's capital and to explore an innovative urban development mode with the priority in eco-environmental protection (Song CQ et al., 2018; Zhu MJ et al., 2019; Ma Z et al., 2021). The New Area is located in the semi-arid North China Plain (NCP), the largest alluvial plain in eastern Asia with serious water shortage problems (Wang SQ et al., 2009). Groundwater has been used as the major water source for drinking, agriculture activities, and industrial productions (Xing LN et al., 2013), and over-exploitation of groundwater has caused numerous changes in groundwater flow conditions and groundwater chemistry (Liu HY et al., 2016), which was caused by the falling groundwater level and the mixture of groundwater in different aquifers. In addition, Xiong'an New Area is home to the NCP's largest natural

First author: *E-mail address*: zhaokai1987924@163.com (Kai Zhao).
* Corresponding author: *E-mail address*: sjzmbh@126.com (Bai-heng Ma); lihaitao@mail.cgs.gov.cn (Hai-tao Li).

doi:10.31035/cg2021058
2096-5192/© 2021 China Geology Editorial Office.

freshwater wetland, Baiyangdian Lake, which plays an important role in the region 's drinking water supply, sustaining agriculture, climate regulation, and flood control (Guo W et al., 2014). Groundwater is of great significance in both maintaining the ecological functions of Baiyangdian Lake and providing the expected water needs of the New Area. In recent decades, intensified human activities have deteriorated the hydrological conditions of the lake (Li X et al., 2016). So far, researches on hydrogeochemistry of the study area have focused on the large spatial scale of the entire NCP (Xing LN et al., 2013; Shi JS et al., 2014; Chen LZ et al., 2014; Liu HY et al., 2015). In Xiong'an New Area and surrounding areas, the systematic and further research on hydrogeochemical characteristics of groundwater in different aquifers under the influence of human activities has not been carried out.

Pore-water is an important site for chemical reactions and frequent material exchanges, which is trapped in particle gaps in terms of bound water, capillary water, and gravity water during sediment deposition (Sacchi E et al., 2001). It is of great significance to identify the hydrogeochemical origin of pore-water in aquitard for revealing the source of elements in groundwater (Zhang YQ et al., 2018; Qaisar M et al., 2020). Sediment pore-water has been used to study the geochemical characteristics of heavy metals (Sadiq R et al., 2003; Zhu H et al., 2011) and the occurrence of gas hydrate (Hesse R, 2003; Cao C and Lei HY, 2012; Sun YB et al., 2012; Valle J et al., 2018). Moreover, pore-water has been utilized to interpret paleoclimate changes and geologic events based on the chemical and isotopic composition (Hendry MJ and Wassenaar LI, 1999; Ortega-Guerrero A, 2003; Hendry MJ and Woodbury AD, 2007; Li J et al., 2014; Niu H et al., 2017; Han DM et al., 2020). As known to all, groundwater plays an important role in global climate change research as the paleoenvironmental information carrier. However, due to the continuous excessive extraction of deep groundwater, groundwater in different aquifers has been intensively mixed, and the paleoclimate information recorded by the aquifer tends to be uniform. The thick clayey layers have the advantage of preserving pore-water, and the transport is dominated by molecular diffusion (Bensenouci F et al. 2014; Hendry MJ and Harrington GA, 2014; Li J et al., 2017). Therefore, pore-water in low-permeability clayey aquitard may be reliable proxy records of paleo-environment relative to aquifer groundwater due to the weaker hydrodynamic alternation.

The groundwater level in Xiong'an New Area has been continuously decreasing due to human activities (Shao JL et al., 2013; Li HT et al., 2021; Ma Z et al., 2021), resulting in groundwater mixture and chemical characteristics change. Therefore, research on hydrogeochemical processes in different aquifers under the influence of human activities in the New Area is the top priority. This study focuses on the sediment pore-water in the Quaternary standard borehole, and aims to (1) horizontally and vertically identify the chemical characteristics and hydrogeochemical processes in the multi-layer aquifer and aquitard system and (2) understand the paleoclimate changes through the analysis of isotopic characteristics of pore-water.

2. Regional background

Xiong'an New Area is located in the east of Taihang Moutain and the central part of the NCP, about 100 km southwest of Beijing, and spans the counties and surrounding areas of Xiongxian, Rongcheng, and Anxin in Hebei Province, covering 1770 km^2 with a population of 2×10^6 to 2.5×10^6 in the long term.

Belonged to the continental monsoon zone with a semi-arid climate, the annual average precipitation and maximum evaporation of the New Area are 478 mm and 1762 mm, respectively. The terrain is relatively flat overall, slightly higher in the west and north, and lower in the east and south. The ground elevation is between 5 m and 20 m, and the slope is between 0.2‰ and 0.7‰. The Quaternary sediments are dominated by alluvial deposits interbedded with lacustrine deposits, and the sediment thickness ranges between 500 m and 600 m (Li HT et al., 2021).

The evolution of palaeogeography and palaeoenvironment during the Quaternary has a direct influence on the formation and evolution of the groundwater system (Zhang ZH et al., 1997). The regional Quaternary groundwater system in Xiong'an New Area consists of four aquifer groups vertically, which is obviously controlled by the lithological distribution and hydraulic features of deposits, corresponding to the Holocene, the upper, the middle, and the lower Pleistocene, respectively (Chen W, 1999; Chen ZY et al., 2003; Shao JL et al., 2013). The thickness of the sediments in each aquifer group gradually increases from the northwest to the southeast of the New Area, and the bottom burial depth of 1^{st}, 2^{nd}, $3^{rd,}$ and 4^{th} aquifer groups is up to 15–35 m, 120–200 m, 280–400 m, and 380–550 m, respectively. The 1^{st} aquifer group is relatively thin and there is a close hydraulic connection between 1^{st} and 2^{nd} aquifer groups. Besides, there are many mixing pumping wells penetrating the two aquifers, resulting in the intensive mixture of groundwater in the first two aquifer groups. Taken together, groundwater in these two aquifers is integrated and assigned as shallow groundwater, which is the main source of water supply for agricultural and industrial usage due to good recoverability. On the other hand, groundwater in the remaining two aquifer groups is referred to as deep groundwater, which is mainly used for the exploitation of domestic water due to good water quality. It is worth noting that deep aquifers have a better water yield property than shallow aquifers.

Generally speaking, both shallow and deep groundwater flow from northwest to southeast under natural conditions (Shao JL et al., 2013; Li HT et al., 2021). The study area has been divided into two zones: Zone 1 and Zone 2, which represent the upstream area and downstream area according to the flow of groundwater in the region, respectively (Fig. 1).

3. Methods and materials

3.1. Groundwater and sediment sampling

One hundred and eighteen groundwater samples were collected from electric-powered public water supply wells in the study area, including seventy-three shallow groundwater

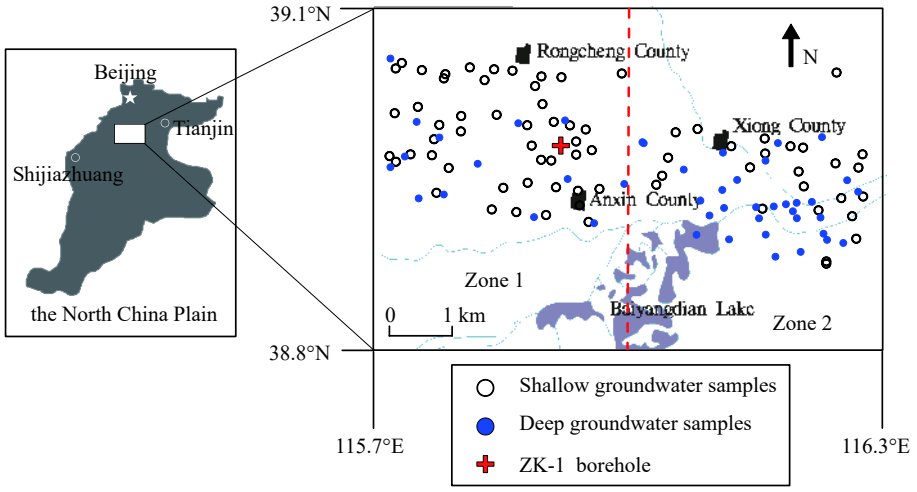

Fig. 1. Sampling locations and the borehole used to sample pore-water in the Xiong'an New Area, North China.

samples and forty-five deep groundwater samples.

All groundwater samples were collected after pumping for more than 20 mins, in order to ensure that the collected groundwater represented water from the aquifer rather than the borehole. All water samples were filtered through 0.22 μm membrane filters. Sampling vessels were acid-washed and deionized water-rinsed thoroughly in the laboratory before the field sampling. Samples for analyzing major cations and trace elements were filtered into 100 mL high-density polyethylene (HDPE) bottles and acidified to pH < 2 by using 6 mol/L purified-HNO_3. Samples for major anions analysis were collected without acidification. All groundwater samples were brought to the laboratory within 3 days and stored at 4°C before analysis.

One representative borehole, located in Zone 1, was drilled to take sediment samples from different aquifers, up to 600 m below land surface. The sampling interval was dependent on lithological settings, and additional samples were collected near lithological boundaries. Eighty-six sediment samples were collected. After sediment removal from the borehole, the internal center parts of the sediment cores were collected to prevent possible contamination. Fresh sediment samples were wrapped in foil and sealed in an N_2-filled plastic bag immediately after sediment sampling. All sediments were transported to the laboratory at 4°C and stored at −20°C in the laboratory until analysis.

3.2. Pore-water extraction

Fifty-seven pore-water samples were extracted from the sediments taken from the borehole in Zone 1 with a depth of 600 m below land surface. The high-speed centrifugation method had been chosen, which was the most widely used technique to obtain pore-water. Compared with squeezing, suction filtration, and dialysis, centrifugation is more accurate and precise for evaluating water chemistry in pore-water (Bufflap SE and Allen HE, 1995; Chapman PM et al., 2002; Zhang Z et al., 2018; Guo HM et al., 2020).

Special Teflon centrifuge tubes were used to extract pore-water by centrifuge under a high speed of 9000 rpm. Specifically, around 25 g of sediment was put in the tube and centrifuged at 9000 rpm for 30 mins at 5°C with a high-speed refrigerated centrifuge (GL21M, Kaida).

After centrifuging, the suspension was filtered by 0.22 μm filter membrane. Samples for analyzing major cations and trace elements were filtered into 10 mL tubes and acidified to pH < 2 by using 6 mol/L purified-HNO_3. The samples for major anions analysis were stored without acidification and all pore-water samples were stored at 4°C before analysis.

3.3. Sample analysis

Groundwater electrical conductivity (EC), temperature (T), pH, and oxidation reduction potential (ORP) were measured *in situ* using a multiparameter probe meter (In-Situ, SMARTROLL MP) with an inline flow cell under minimal atmospheric contact. Concentrations of major cations and trace elements were detected by ICP-AES (iCAP6000, Thermo) and ICP-MS (7500C, Agilent), respectively, with an analytical precision of 0.5%. Major anions, including NO_3^-, Cl^-, SO_4^{2-}, and F^-, were determined using ion chromatography (ICS2000, Dionex) with an analytical precision of less than 3.0%. Ion charge imbalances were less than 10% for all samples.

The oxygen and hydrogen stable isotopes were performed by using L2120-ianalyzer (Picarro, USA). These isotopic ratios of D/H and $^{18}O/^{16}O$ are expressed as δ notation [δ = 1000 ($R_{Sample}/R_{Standard}-1$)] with respect to the VSMOW (Vienna Standard Mean Ocean Water) international standard. Analytical precisions of $\delta^{18}O$ and δD were ±0.2‰ and ±1‰, respectively.

4. Results and discussion

4.1. Major components of groundwater and pore-water

Groundwater in the Xiong'an New Area was neutral to weakly alkaline, with the pH between 6.7 and 9.5 (median, 7.7) and between 7.2 and 8.6 (median, 8.2) in shallow and deep aquifers, respectively (Table 1). Na^+ was the dominant cation, and HCO_3^- was the major anion in both shallow and deep groundwater. The total dissolved solids (TDS) varied greatly in different aquifers, with the ranges between 264 mg/L and 6478 mg/L (median, 1003 mg/L) and between 264

Table 1. Statistic results of physiochemical parameters of groundwaters in the Xiong'an New Area, North China.

	Unit	Shallow groundwater in Zone 1 (n = 45)			Shallow groundwater in Zone 2 (n = 28)			Deep groundwater in Zone 1 (n = 12)			Deep groundwater in Zone 2 (n = 33)		
		Max	Min	Mean	Max	Min	Mean	Max	Min	Mean	Max	Min	Mean
Depth	m	150	50	84	120	15	73	500	200	312	580	180	287
pH		9.5	6.7	7.6	9.4	6.7	7.8	8.4	7.6	8.2	8.6	7.2	8.4
TDS	mg/L	4502	269	977	6478	264	1045	480	280	387	1342	264	465
K^+	mg/L	24.9	<0.5	2.1	3.7	<0.5	1.2	1.7	<0.5	1.0	1.9	<0.5	0.4
Na^+	mg/L	753.0	18.8	151.2	1096.0	27.4	213.6	105.3	39.1	83.3	223.0	86.5	133.0
Ca^{2+}	mg/L	198.2	11.4	79.6	422.9	3.2	69.9	41.9	8.9	18.5	89.4	3.2	11.1
Mg^{2+}	mg/L	348.8	8.8	69.2	429.1	1.0	57.1	20.0	2.0	10.8	60.6	<0.5	4.3
Cl^-	mg/L	526.3	5.6	100.5	843.8	11.3	146.3	46.6	5.6	27.3	177.8	15.5	50.3
SO_4^{2-}	mg/L	2503.0	11.5	240.7	3235.0	22.4	298.4	43.4	26.8	32.4	268.9	23.6	49.5
NO_3^-	mg/L	75.5	<0.5	14.6	13.7	<0.5	3.2	19.2	<0.5	10.2	3.9	<0.5	0.7
HCO_3^-	mg/L	799.2	84.7	481.8	893.8	120.0	417.7	284.7	162.3	217.9	625.6	188.2	235.2

mg/L and 1342 mg/L (median, 444 mg/L) in shallow and deep groundwater, respectively. Shallow groundwater had a higher value of TDS relative to deep groundwater, including all major ions except K^+. The concentration of K^+ in groundwater was low and remained stable throughout. For the major anions, SO_4^{2-} concentrations were comparable to those of Cl^- in shallow groundwater, while SO_4^{2-} concentrations were lower than those of Cl^- in deep groundwater. Relatively higher NO_3^- concentrations (median, 3.51 mg/L) were observed in shallow groundwater compared to deep groundwater (median, 0.84 mg/L), but around 30% of deep groundwater samples had NO_3^- concentrations greater than 5.0 mg/L.

Along the direction of groundwater runoff, there was no obvious change overall. Nevertheless, there was an upward trend in Na^+ concentration and a downward trend in Ca^{2+} and Mg^{2+} concentrations in both shallow and deep groundwater from Zone 1 to Zone 2 (Fig. 2), indicating the occurrence of ion exchange processes along the flow path in the aquifers. In addition, the concentrations Cl^- and SO_4^{2-} increased along with the groundwater runoff due to the leaching effect.

The major components of pore-water samples were listed in Table 2. Pore-water was near-neutral to weak alkaline (7.50 –8.36 in shallow aquifers and 7.49 –8.53 in deep aquifers). The pore-water samples had TDS values from 267 mg/L to 868 mg/L (median, 413 mg/L) and from 243 mg/L to 662 mg/L (median, 387 mg/L) in shallow and deep aquifers, respectively. The high TDS values mostly occurred in aquifers with a depth around 50–70 m and >500 m below land surface. In general, shallow pore-water had fewer Na^+, but more Ca^{2+} and Mg^{2+}, compared with deep pore-water. Na^+ was the dominant cation with a range of 38.16 mg/L to 397.47 mg/L (median value: 124.12 mg/L) and 72.12 mg/L to 263.38 mg/L (median value: 148.17 mg/L) in shallow and deep aquifers, respectively. Meanwhile, HCO_3^- was the major anion in both shallow and deep pore-water, with concentrations up to 587.21 mg/L and 415.91 mg/L, respectively. Besides, low NO_3^- concentrations (<20 mg/L) were observed in pore-water from both shallow and deep aquifers.

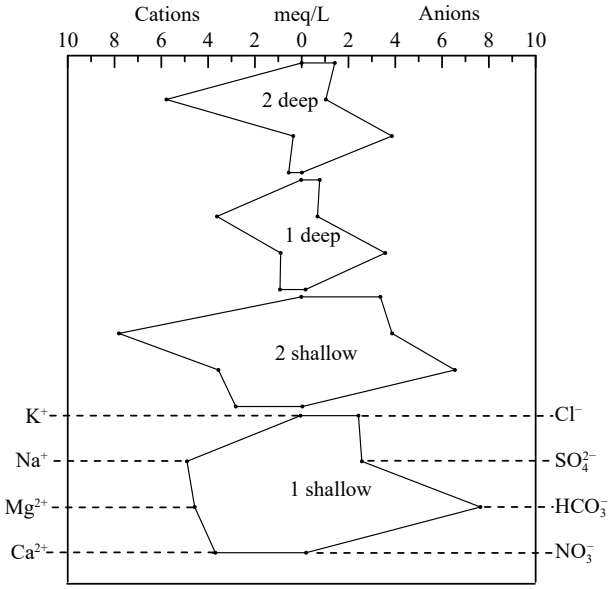

Fig. 2. Stiff plots of groundwater in the Xiong'an New Area, North China. 1 shallow–shallow groundwater in Zone 1; 2 shallow–shallow groundwater in Zone 2; 1 deep–deep groundwater in Zone 1; 2 deep–deep groundwater in Zone 2.

The parameters of pore-water were compared with those of groundwater in Zone 1 because of the location factor. Although both Na^+ and Cl^- concentrations were higher in deep pore-water than in coexisting groundwater, concentrations of Ca^{2+}, Mg^{2+}, SO_4^{2-}, and HCO_3^- in deep pore-water were similar to those in coexisting groundwater. In contrast, the concentrations of all major ions in shallow groundwater were much higher than those in shallow pore-water. For example, shallow pore-water had NO_3^- concentrations between 3.38 mg/L and 9.92 mg/L (median, 6.11 mg/L), which were mostly lower than the coexisting shallow groundwater.

As shown in Fig. 3, the distribution of major components of pore-water and groundwater in Zone 1 at different depths was approximately consistent. Furthermore, the scatter points of major components of pore-water in different aquifers were clustered in or close to the box-whisker plot of the groundwater in Zone 1 at the corresponding depths through further analysis.

Table 2. Statistic results of physiochemical parameters of pore-water in aquifer sediments of ZK-1 borehole in the Xiong'an New Area, North China.

	Unit	Shallow pore-water (n = 16)			Deep pore-water (n = 41)		
		Max	Min	Mean	Max	Min	Mean
Depth	m	143.0	22.5	81.6	557.4	151.0	365.3
pH		8.36	7.50	8.06	8.53	7.49	8.27
TDS	mg/L	868	267	413	662	243	387
K^+	mg/L	14.54	1.59	4.16	3.46	0.78	1.92
Na^+	mg/L	397.47	38.16	124.12	263.38	72.12	148.17
Ca^{2+}	mg/L	88.27	22.66	38.99	38.76	5.49	16.48
Mg^{2+}	mg/L	36.50	13.14	22.94	22.52	2.20	8.22
Cl^-	mg/L	352.08	38.88	97.32	196.94	22.90	78.87
SO_4^{2-}	mg/L	217.50	210.78	76.34	67.27	26.08	41.66
NO_3^-	mg/L	9.92	3.38	6.11	20.38	<0.50	8.36
HCO_3^-	mg/L	587.21	90.81	296.90	415.91	171.06	288.53

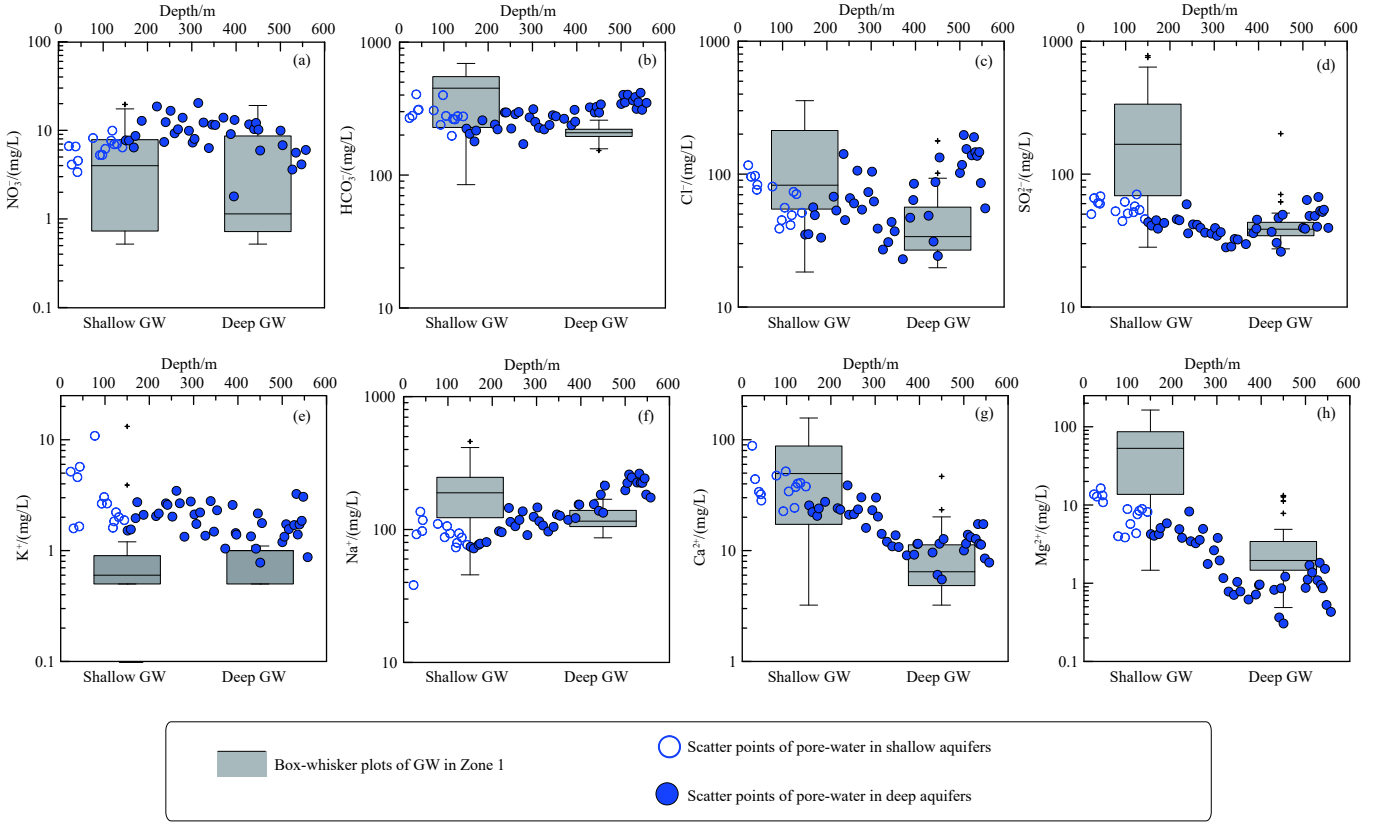

Fig. 3. Box-whisker plots of major ions in shallow and deep groundwater in Zone 1 and depth-dependent concentrations of major components of pore-water in the Xiong'an New Area, North China.

Due to severe groundwater overexploitation, most of the groundwater samples collected in the piloted wells were strongly mixed in the NCP, which could lead to confusing components. However, the pore-water accurately corresponded to the specific aquifer, eliminating the influence of groundwater mixture from different depths during pumping. The aquifer pore-water was more accurate and representative than the groundwater collected in the region. Therefore, the pore-water is recommended to analyze the hydrochemistry characteristics relative to groundwater, which is more helpful to the fine description of the hydrogeochemical process in the study area.

4.2. Hydrogeochemical characteristics of groundwater and pore-water

As seen from the Piper plot in Fig. 4a, the type of water chemistry did not change obviously along the direction of groundwater runoff (from Zone 1 to Zone 2), which might result from a short runoff path. However, the types of groundwater chemistry in deep and shallow aquifers were quite different. From the shallow aquifer to the deep aquifer, the milligram equivalent percentage of Na+K increased to about 90%, and the chemical type of groundwater changed from mixed type to $HCO_3 \cdot SO_4$-Na type. The samples of

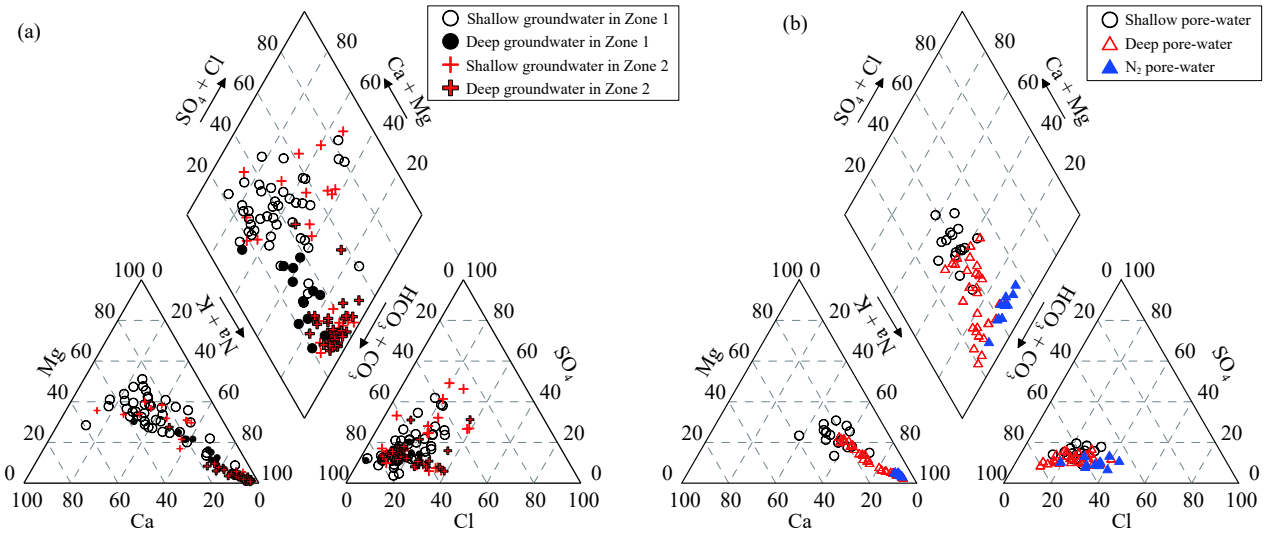

Fig. 4. Piper plots of groundwater (a) and pore-water (b) in the Xiong'an New Area, North China.

shallow groundwater were characterized by multiple hydrochemical facies, such as $HCO_3 \cdot SO_4$-Na(Ca) and $HCO_3 \cdot$Cl-Na(Mg).

Similarly, the same vertical variation characteristics of groundwater chemical types could be obtained more clearly from the Piper plot of pore-water in Fig. 4b. The shallow pore-water samples were located in the middle of the Piper plot, which represented the mixed type of water chemistry. However, the deep pore-water samples for N_2 sediments were located in the lower right corner, which represented the $HCO_3 \cdot SO_4$-Na type. As the depth increased, the pore-water in the middle layer transited to the lower right in turn. It is worth noting that the change process of cations in different layers with depth was particularly significant. The content of Na ions gradually increased with the increase in depth, which caused the position of pore-water samples on the Piper plot to shift gradually from the middle to the lower right. In addition, it can be seen from Fig. 4b that the pore-water samples extracted from different lithological sediments at the adjacent depth were located in similar positions in the Piper plot, indicating that there was no significant difference in their water chemistry types.

4.3. Hydrogeochemical processes in different aquifers

As an indispensable method, the Gibbs plot is widely used to qualitatively analyze the hydrogeochemical processes in a certain area (Gibbs RJ, 1970). The water chemistry data of groundwater and pore-water samples were respectively placed on the Gibbs plot according to depth and runoff, as shown in Fig. 5. The samples of groundwater and pore water were distributed in the zone between rock weathering and evaporation-crystallization, indicating that the major components of groundwater and pore-water did not possess the hydrogeochemical characteristics of meteoric water. After receiving the replenishment of meteoric water to the aquifer, it experienced a long time of water-rock interaction.

As shown in Fig. 5a, the distribution of groundwater in Zone 1 and Zone 2 in the Gibbs plot was basically the same, indicating that the hydrogeochemical process of groundwater was consistent along the direction of groundwater runoff. However, the distribution of shallow and deep groundwater was quite different. Shallow groundwater was distributed in the upper middle part of the Gibbs plot, and the value of Na/(Na+Ca) was between 0.4 and 0.8. The TDS value was slightly higher than that of the deep water, indicating that the shallow groundwater was mainly affected by evaporative crystallization and rock weathering. Whereas, deep groundwater was distributed in the middle right part of the Gibbs plot, and the value of Na/(Na+Ca) was close to 1, representing the combined influence of the three effects of evaporation-crystallization, rock weathering, and atmospheric precipitation. Furthermore, in the Gibbs plot of Fig. 5b, shallow groundwater in Zone 1 was distributed at the upper left of the shallow pore-water, indicating that shallow groundwater was more concentrated by evaporation than pore-water. Meanwhile, both deep groundwater and pore-water were distributed in the middle right part, indicating similar hydrogeochemical processes.

The water-rock interaction plays an important role in the evolution of major solute compositions in groundwater. Because Cl and Br are ubiquitous in natural water, as well as their conservative behavior and high solubility, processes such as ion exchange reaction and mineral surface adsorption cannot significantly change the concentration of Cl and Br. The water-rock interaction generally causes the dissolution of halite (NaCl) in sediments, which would directly lead to an increase in the concentration of chloride ions, thereby causing a rapid increase in the Cl/Br ratio. In contrast, the evaporation process can change the absolute concentration of Cl and Br in the groundwater, but not the Cl/Br ratio before the groundwater reaches the saturation of halite. Therefore, the concentration of chloride ions and Cl/Br ratio are frequently used to identify and distinguish the evolution process of lixiviation and evaporation (Cartwright I et al, 2006; Deng YM et al, 2009; Xing LN et al, 2013; Taheri M et al, 2017).

It is seen from Fig. 6 that the Cl/Br ratio of deep groundwater in Zone 1 and Zone 2 increased rapidly with the

increase of chloride ion concentration, and the deep groundwater samples clustered nearly along the trend line of halite dissolution. However, the change of the Cl/Br ratio was not obvious in shallow groundwater. The above results suggested that halite dissolution and evaporative concentration played a greater role in the hydrogeochemical process of the deep and shallow aquifer, respectively. Meanwhile, pore-water had basically the same changing law as groundwater in Zone 1, and the difference was mainly in the deep pore-water samples for N_2 sediments. Due to the relatively dry and hot climate conditions in the Neogene period, pore-water in the N_2 layer was more affected by evaporation, which could be confirmed by the results of stable oxygen and hydrogen isotopes.

4.4. Characteristics of stable oxygen and hydrogen isotopes

Stable oxygen and hydrogen isotope relationships of pore-water in different lithological sediments in the study area are shown in Table 3 and Fig. 7. Aquifer pore-water had $\delta^{18}O$ between −11.4 ‰ and −7.6 ‰ (median, −10.6 ‰) and δD between −84.0 ‰ and −59.6 ‰ (median, −77.0 ‰), while aquitard pore-water had $\delta^{18}O$ between −10.6 ‰ and −6.5 ‰ (median, −10.0 ‰) and δD between −80.2 ‰ and −52.6 ‰ (median, −74.2‰).

The $\delta^{18}O$ and δD values of aquifer pore-water were associated with the global meteoric water line (GMWL), and the fitting equation was $\delta D = 6.16\delta^{18}O - 12.37$ (R^2=0.95). According to the general-purpose diagram of δD versus $\delta^{18}O$ with total 13 trend lines to trace the water origin and reveal the various processes (Pang ZH et al., 2017), aquifer pore-water mostly originated from meteoric water under the influence of evaporation. Meanwhile, the $\delta^{18}O$ and δD values of most shallow pore-water were more positive than those of deep pore-water, which coincided with previous studies on the

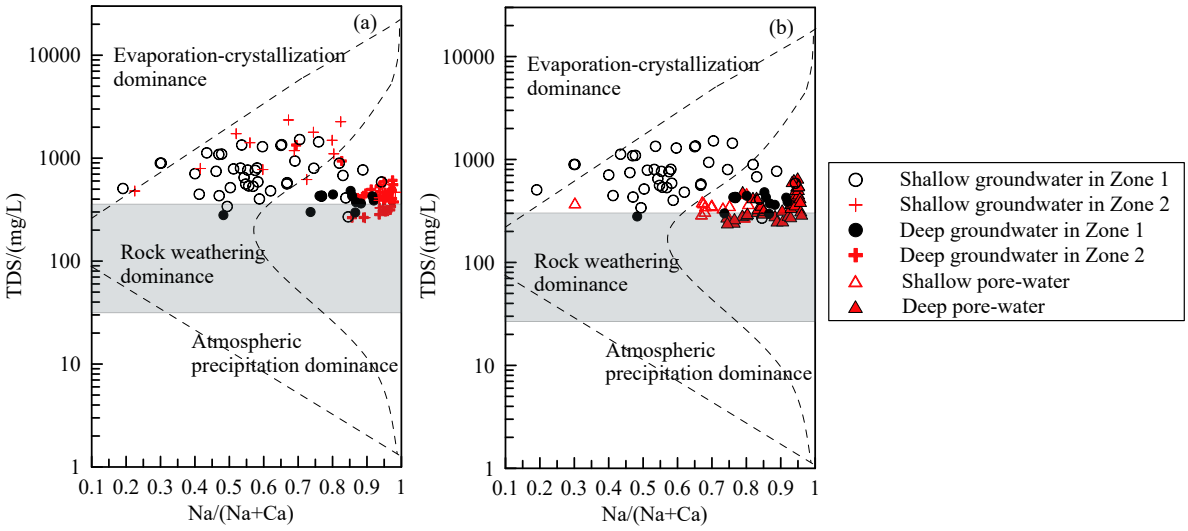

Fig. 5. Gibbs plots of groundwater (a) and pore-water (b) in the Xiong'an New Area, North China.

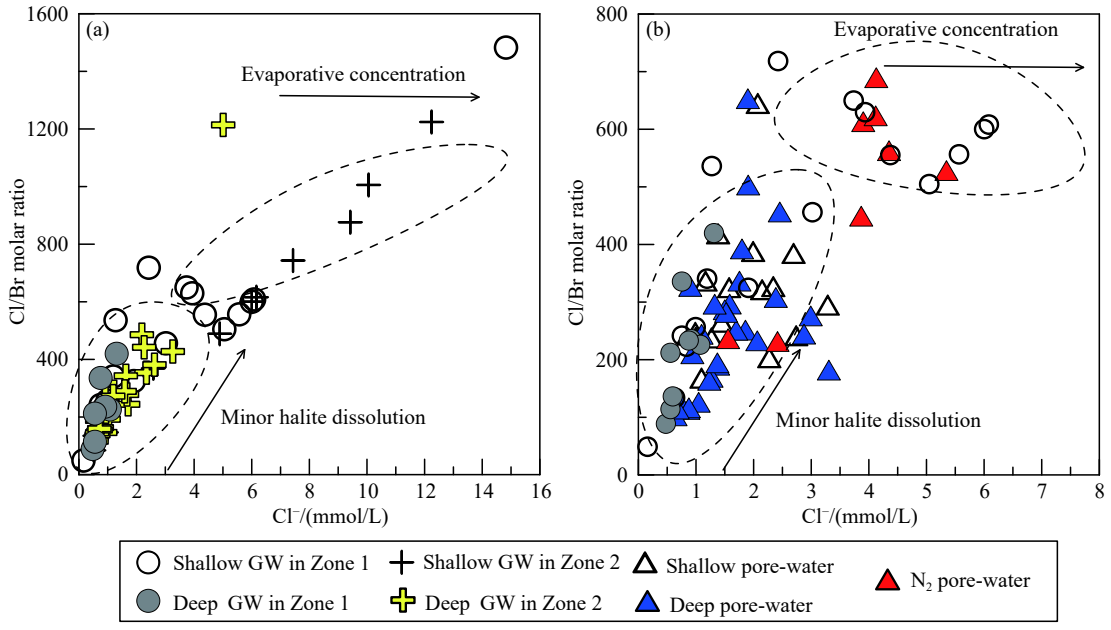

Fig. 6. Variations in Cl/Br ratios with Cl concentration of groundwater (a) and pore-water (b) in the Xiong'an New Area, North China.

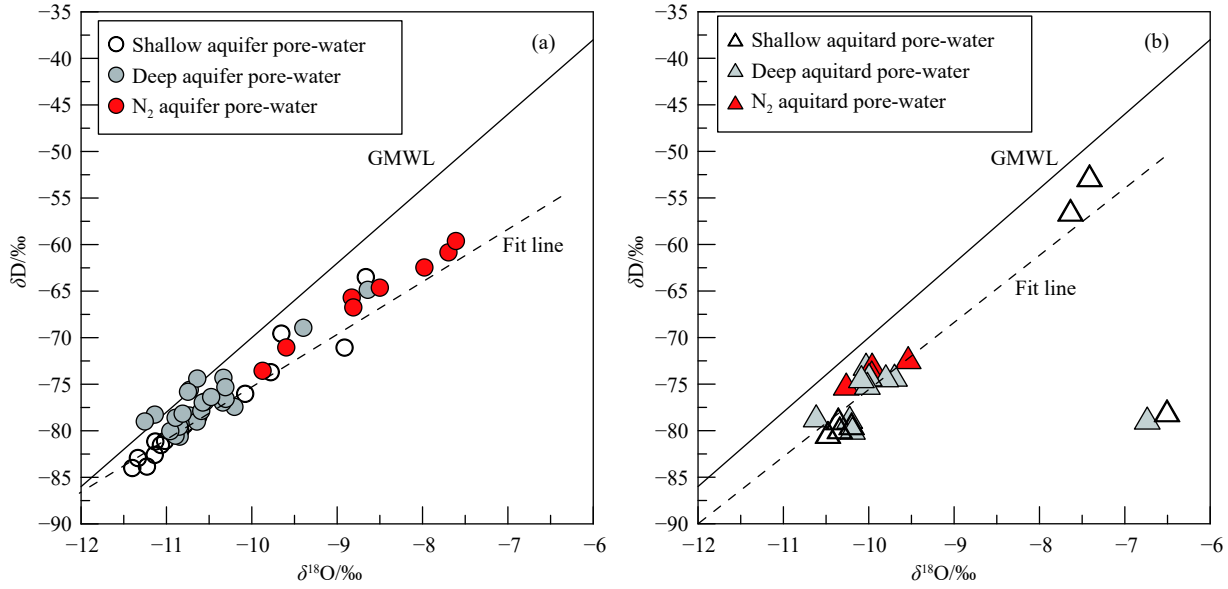

Fig. 7. Stable isotopic composition of aquifer pore-water (a) and aquitard pore-water (b) in the Xiong'an New Area, North China. The solid line marks the global meteoric water line (GMWL).

Table 3. Stable isotopic composition of pore-water in sediments of ZK-1 borehole in the Xiong'an New Area, North China

Pore-water	Sample No.	Depth/m	$\delta^{18}O$/‰	δD/‰	Pore-water	Sample No.	Depth/m	$\delta^{18}O$/‰	δD/‰
Aquifer pore-water	ZK-1-14	22.5	−8.66	−63.50		ZK-1-284	445.0	−10.73	−75.60
	ZK-1-20	29.0	−9.65	−69.56		ZK-1-287	450.4	−11.25	−79.00
	ZK-1-29	37.8	−8.91	−71.07		ZK-1-313	500.3	−10.64	−74.39
	ZK-1-33	41.9	−9.78	−73.71		ZK-1-315	505.0	−10.75	−75.81
	ZK-1-35	43.1	−11.02	−81.09		ZK-1-317	509.0	−8.64	−64.86
	ZK-1-61	77.1	−10.08	−76.03		ZK-1-319	515.0	−8.50	−64.63
	ZK-1-74	92.7	−11.40	−84.00		ZK-1-326	527.0	−7.98	−62.46
	ZK-1-80	98.1	−11.23	−83.85		ZK-1-329	532.0	−8.83	−65.69
	ZK-1-84	104.8	−10.63	−78.49		ZK-1-331	535.0	−7.70	−60.83
	ZK-1-96	117.9	−11.14	−82.59		ZK-1-333	539.0	−8.81	−66.75
	ZK-1-98	120.7	−11.13	−81.15		ZK-1-336	544.0	−7.61	−59.62
	ZK-1-101	124.9	−10.84	−79.99		ZK-1-338	547.5	−9.60	−71.05
	ZK-1-104	131.2	−10.79	−79.35		ZK-1-343	557.4	−9.87	−73.56
	ZK-1-113	143.5	−11.07	−81.53	Aquitard pore-water	ZK-1-06	9.7	−7.41	−52.60
	ZK-1-127	158.3	−11.33	−82.92		ZK-1-10	15.9	−7.64	−56.30
	ZK-1-134	169.1	−10.73	−78.36		ZK-1-16	24.8	−10.20	−74.25
	ZK-1-148	187.0	−10.20	−77.43		ZK-1-44	54.3	−10.36	−78.71
	ZK-1-164	215.3	−10.34	−76.96		ZK-1-67	84.5	−10.48	−80.18
	ZK-1-167	221.3	−10.85	−80.63		ZK-1-100	123.5	−10.34	−79.68
	ZK-1-176	237.6	−9.40	−68.94		ZK-1-110	139.6	−6.51	−77.85
	ZK-1-200	279.3	−10.89	−80.53		ZK-1-132	165.0	−10.09	−74.20
	ZK-1-207	293.5	−10.64	−79.01		ZK-1-142	179.2	−10.62	−78.40
	ZK-1-211	301.9	−10.33	−74.31		ZK-1-169	225.5	−10.19	−79.73
	ZK-1-214	306.2	−10.59	−77.87		ZK-1-183	248.2	−10.22	−78.56
	ZK-1-219	314.6	−10.84	−79.24		ZK-1-189	258.6	−6.74	−78.64
	ZK-1-225	326.5	−10.85	−79.56		ZK-1-221	319.2	−10.02	−74.91
	ZK-1-231	338.5	−10.96	−80.04		ZK-1-251	379.8	−10.00	−74.01
	ZK-1-235	346.0	−10.55	−76.87		ZK-1-263	406.5	−10.03	−72.86
	ZK-1-238	353.0	−10.89	−78.60		ZK-1-272	424.5	−10.00	−74.01
	ZK-1-247	371.4	−10.81	−78.16		ZK-1-285	447.0	−9.80	−74.10
	ZK-1-254	388.0	−10.31	−76.57		ZK-1-307	487.2	−9.70	−74.03
	ZK-1-258	395.0	−10.31	−75.32		ZK-1-356	589.8	−9.96	−72.85
	ZK-1-259	396.5	−10.58	−76.96		ZK-1-358	595.3	−9.54	−72.15
	ZK-1-276	429.5	−10.48	−76.38		ZK-1-359	598.0	−10.26	−74.99
	ZK-1-282	440.7	−11.14	−78.26		ZK-1-360	599.6	−9.97	−73.69

stable oxygen and hydrogen isotopes of groundwater in the North China Plain (Xing LN et al., 2013). This implies that either (1) groundwater recharge into the deep aquifer took place in a higher altitude zone with lower $\delta^{18}O$ and δD in precipitation, and deep groundwater was mainly recharged from high altitudes of the Taihang Mountains in the northwest; or (2) deep groundwater reflects older groundwater from *in situ* recharge during times of higher precipitation and/or lower temperature (Guo HM et al., 2020). In addition, the $\delta^{18}O$ and δD values of N_2 pore-water were obviously positive, which was consistent with the warm climate of the Pliocene.

For aquitard pore-water, the fitting line was almost parallel to the GMWL, and the fitting equation was $\delta D = 8.22\delta^{18}O + 7.46$ ($R^2 = 0.95$), suggesting that aquitard pore-water belonged to Paleo meteoric water. The $\delta^{18}O$ and δD values of some shallow aquitard pore-water were lower than those of deep aquitard pore-water. This might be caused by the relatively mild and humid climate at that time, and the heavy rainfall made the oxygen and hydrogen isotope values depleted.

4.5. Response of pore-water isotope characteristics to paleoclimate changes

The isotope characteristics can show the change of the research area as a climate and environment index. The $\delta^{18}O$ profiles of pore-water for different lithological sediments were used to analyze the response to paleoclimate changes in this manuscript, which was shown in Fig. 8. It is worth noting that the geological age at the depth of 600 m at the bottom of the representative borehole was inferred from the comparion between sediment paleomagnetic data and standard geomagnetic polarity time scale, which was a relative age of circa 3.10 Ma BP. Based on the $\delta^{18}O$ profiles of pore-water and sporopollen records from sediments at different depths, the characteristics of paleoclimatic zoning in the study area were comprehensively inferred as follows.

(i) Paleoclimatic Zone I_b (600–490 m): The $\delta^{18}O$ values of pore-water fluctuated significantly, with an average value of −9.93‰. At the same time, the numbers of sporopollen grains were generally low, and the herbal and woody sporopollen appeared alternately during this period. Both $\delta^{18}O$ values and sporopollen records reflected a climate change process of dry and cold to warm and humid.

(ii) Paleoclimatic Zone I_a (490–387 m): The $\delta^{18}O$ values of aquitard pore-water remained basically stable, with an average value of −9.88 ‰. The aquitard pore-water was slightly enriched in $\delta^{18}O$ relative to the corresponding aquifer pore-water and the aquitard pore-water in Zone I_b. In the meanwhile, the total number of sporopollen grains in this period had an increasing trend relative to Zone I_b, indicating the warm and humid climate conditions in Pliocene. Specifically speaking, the numbers of herbal sporopollen decreased, while those of woody sporopollen increased.

(iii) Paleoclimatic Zone II (387–15.8 m): Overall, the $\delta^{18}O$ values of aquitard pore-water were a bit more negative than those in Zone I, with an average value of −10.3‰ (excluding the abnormal points at 258 m and 139 m). Also, the numbers of sporopollen grains were generally low, and the pollen content of herbaceous plants was much higher than that of woody plants, reflecting the relatively low temperature and arid climate since the Quaternary Period. It is worth noting that the $\delta^{18}O$ values had two obvious rises under the overall negative condition, corresponding to the peaks at 258 m and 139 m, respectively, indicating the warm and dry climate in the Quaternary interglacial period. Furthermore, there were also two higher $\delta^{18}O$ values at 237 m and 77 m in the aquifer pore-water. The response magnitude was not obvious and the depth was shifted relative to the aquitard pore-water, which might be caused by the mixing of pore-water in different aquifers under the condition of groundwater overexploitation.

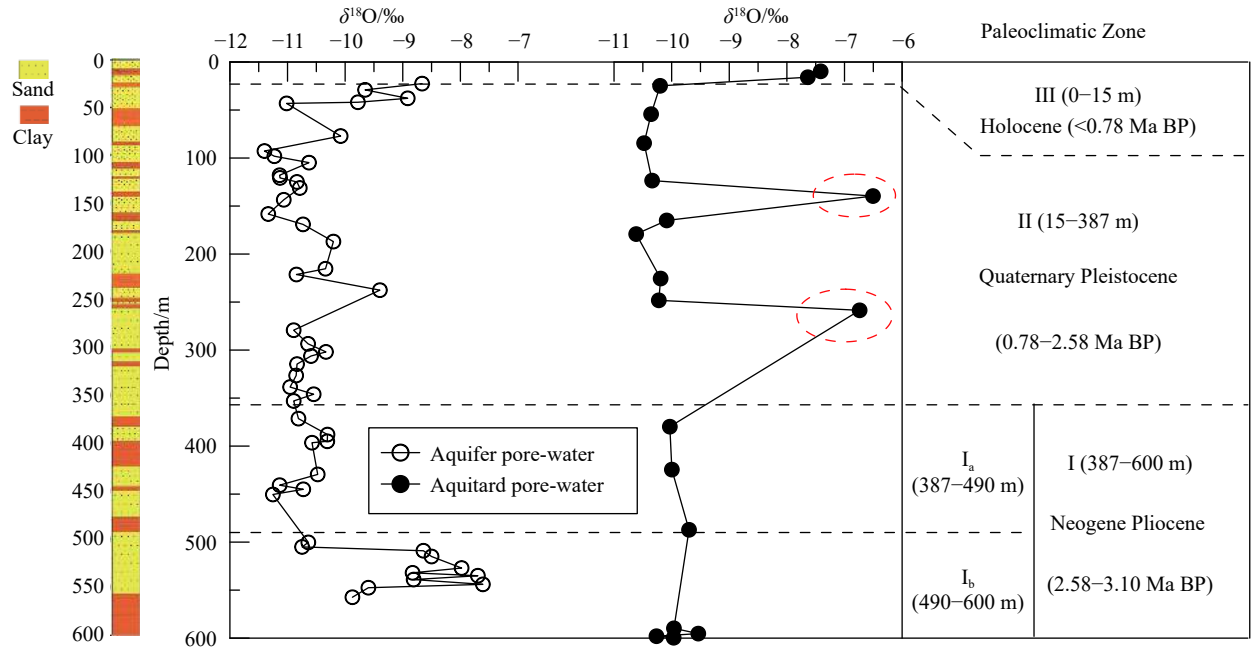

Fig. 8. The $\delta^{18}O$ profiles of pore-water and paleoclimate significance in the Xiong'an New Area, North China.

(iv) Paleoclimatic Zone III (15.8–0 m): The $\delta^{18}O$ values of aquitard and aquifer pore-water significantly increased, and the corresponding average values were −7.53‰ and −8.66‰, respectively. This is consistent with the warm and humid climate of the Holocene reflected by the apparent increase in the total number of sporopollen grains and the appearance of a large number of woody and fern plants.

As can be seen from the above, due to the mixing of pore-water in different aquifers, the isotope values of aquifer pore-water are not timely and accurate to respond to climate changes as the same as groundwater in the groundwater over-extracted area. Compared with aquifer pore-water and groundwater, aquitard pore-water had a more closed environment and slower hydrodynamic conditions, so that aquitard pore-water could more completely retain the feature of paleo-sedimentary water (Harrington GA et al., 2013; Li J et al., 2014; Han DM et al., 2020). As a direct record, the isotope of aquitard pore-water can intuitively respond to paleoclimate changes.

5. Conclusions

This study focuses on the analysis of the similarities and differences between groundwater and sediment pore-water in Xiong'an New Area, as well as the $\delta^{18}O$ profiles of pore-water and sporopollen records from sediments at different depths, and the main conclusions are as follows:

(i) Both groundwater and pore-water were neutral to weakly alkaline, with the dominant components of Na^+ and HCO_3^-. The major components and chemical type of groundwater did not change significantly along the direction of groundwater runoff but obviously changed with depth. Deep groundwater was predominantly $HCO_3 \cdot SO_4$-Na type, whereas shallow groundwater was characterized by multiple hydrochemical facies. Shallow groundwater (<150 m) had a higher value of TDS than a deep one, including all major ions except K^+. The high salinity and elevated NO_3^- in the shallow groundwater suggest modern recharge with some anthropogenic contamination (e.g., agricultural irrigation). In comparison, deep groundwater has better water quality but is vulnerable to contamination from shallow groundwater with high TDS and NO_3^- concentrations.

(ii) Different hydrochemical processes occurred in shallow and deep groundwater. Shallow groundwater was influenced by evaporation, carbonate dissolution, and silicate weathering, while evaporite dissolution and silicate weathering played an important role in the deep aquifer. Cation exchange occurred as well in all aquifers. Moreover, pore-water has similar major components and hydrogeochemical processes with groundwater in Zone 1, which demonstrates the possibilities of the applications of pore-water on the hydrogeochemical study.

(iii) The values of pore-water oxygen isotope are positive in the warm climate, and aquitard pore-water has a more significant response to climate change relative to aquifer pore-water. The evolution of paleo-vegetation and paleo-climate since 3.10 Ma BP was reconstructed by analyzing the results of sporopollen and isotope: (1) The climate in the Neogene Pliocene (2.58–3.10 Ma BP) was relatively warm and humid; (2) the Quaternary Pleistocene (0.78 –2.58 Ma BP) was dominated by the cold and dry climate of the glacial period, with three interglacial intervals of warm and humid climate; (3) the climate has become significantly warmer since the Holocene (<0.78 Ma BP).

CRediT authorship contribution statement

Kai Zhao and Jing-xian Qi conceived of the presented idea and finished the main part of the manuscript. Yi Chen was responsible for field sampling and analyzed the field data. Hua-ming Guo and Hai-tao Li put forward suggestions and opinions on the structure of the article and supervised the finding of this work. Bai-heng Ma, Li Yi, Xin-zhou Wang, and Lin-ying Wang provided a lot of help for on-site sampling and laboratory sample testing. All authors discussed the results and contributed to the final manuscript.

Declaration of competing interest

The authors declare no conflict of interest.

Acknowledgment

The study was financially supported by the National Natural Science Foundation of China (41807220), the Open Fund Project of Hebei Key Laboratory of Geological Resources and Environment Monitoring and Protection (JCYKT201903), and the projects of the China Geological Survey (DD20160239 and DD20189142). Thanks for the hard work of the editors and the constructive suggestions from the peer reviewers.

References

Bensenouci F, Michelot JL, Matray JM, Savoye S, Massault M, Vinsot A. 2014. Coupled study of water-stable isotopes and anions in porewater for characterizing aqueous transport through the Mesozoic sedimentary series in the eastern Paris Basin. Marine and Petroleum Geology, 53, 88–101. doi: 10.1016/j.marpetgeo.2013.12.012.

Bufflap SE, Allen HE. 1995. Sediment pore water collection methods for trace metal analysis: A review. Water Research, 29(1), 165–177. doi: 10.1016/0043-1354(94)E0105-F.

Cao C, Lei HY. 2012. Geochemical characteristics of pore water in shallow sediments from north continental slope of South China Sea and their significance for natural gas hydrate occurrence. Procedia Environmental Sciences, 12(PartB), 1017–1023. doi: 10.1016/j.proenv.2012.01.381.

Cartwright I, Weaver T, Fifield L. 2006. Cl/Br ratios and environmental isotopes as indicators of recharge variability and groundwater flow: An example from the southeast Murray Basin, Australia. Chemical Geology, 231(1−2), 38–56. doi: 10.1016/j.chemgeo.2005.12.009.

Chapman PM, Wang FY, Germano JD, Batley G. 2002. Pore water testing and analysis: The good, the bad, and the ugly. Marine Pollution Bulletin, 44(5), 359–366. doi: 10.1016/S0025-326X(01)00243-0.

Chen LZ, Ma T, Du Y, Yang J, Liu L, Shan HM, Liu CF, Cai HS. 2014. Origin and evolution of formation water in North China Plain based on hydrochemistry and stable isotopes (^2H, ^{18}O, ^{37}Cl and ^{81}Br). Journal of Geochemical Exploration. 145, 250–259. doi: 10.1016/j.gexplo.2014.07.006.

Chen W. 1999. Groundwater in Hebei Province. Beijing, Seismological Press, 41–55 (in Chinese).

Chen ZY, Qi JX, Xu JM, Xu JM, Ye H, NanYJ. 2003. Paleoclimatic interpretation of the past 30 ka from isotopic studies of the deep confined aquifer of the North China plain. Applied Geochemistry, 18(7), 997–1009. doi: 10.1016/S0883-2927(02)00206-8.

Deng YM, Wang YX, Ma T. 2009. Isotope and minor element

geochemistry of high arsenic groundwater from Hangjinhouqi, the Hetao Plain, Inner Mongolia. Applied Geochemistry, 24(4), 587–599. doi: 10.1016/j.apgeochem.2008.12.018.

Gibbs RJ. 1970. Mechanisms controlling world water chemistry. Science, 170(3962), 1088–1090. doi: 10.1126/science.170.3962.1088.

Guo HM, Chen Y, Hu HY, Zhao K, Li HT, Yan S, Xiu W, Coyte RM, Vengosh A. 2020. High hexavalent chromium concentration in groundwater from a deep aquifer in the Baiyangdian Basin of the North China Plain. Environmental Science and Technology, 54(16), 10068–10077. doi: 10.1021/acs.est.0c02357.

Guo W, Zhang HY, Huo SL. 2014. Organochlorine pesticides in aquatic hydrophyte tissues and surrounding sediments in Baiyangdian wetland, China. Ecological Engineering, 67, 150–155. doi: 10.1016/j.ecoleng.2014.03.047.

Han DM, Cao GL, Currell MJ, Priestley SC, Love AJ. 2020. Groundwater salinization and flushing during glacial-interglacial cycles: Insights from aquitard porewater tracer profiles in the North China Plain. Water Resources Research, 56(11). doi: 10.1029/2020WR027879.

Harrington GA, Gardner WP, Smerdon BD, Hendry MJ. 2013. Palaeohydrogeological insights from natural tracer profiles in aquitard porewater, Great Artesian Basin, Australia. Water Resources Research, 49(7), 4054–4070. doi: 10.1002/wrcr.20327.

Hendry MJ, Harrington GA. 2014. Comparing vertical profiles of natural tracers in the Williston Basin to estimate the onset of deep aquifer activation. Water Resources Research, 50(8), 6496–6506. doi: 10.1002/2014WR015652.

Hendry MJ, Wassenaar LI. 1999. Implications of the distribution of δD in pore waters for groundwater flow and the timing of geologic events in a thick aquitard system. Water Resources Research, 35(6), 1751–1760. doi: 10.1029/1999WR900046.

Hendry MJ, Woodbury AD. 2007. Clay aquitards as archives of Holocene paleoclimate: δ^{18}O and thermal profiling. Groundwater, 45(6), 683–691. doi: 10.1111/j.1745-6584.2007.00354.x.

Hesse R. 2003. Pore water anomalies of submarine gas-hydrate zones as tool to assess hydrate abundance and distribution in the subsurface: What have we learned in the past decade? Earth-Science Reviews, 61(1), 149–179. doi: 10.1016/S0012-8252(02)00117-4.

Li HT, Feng W, Wang KL, Zhao K, Li G, Zhang Y, Li MZ, Sun L, Chen YC, You B. 2021. Groundwater resources in Xiong'an New Area and its exploitation potential. Geology in China, 48(4), 1112–1126 (in Chinese with English abstract). doi: 10.12029/gc20210409.

Li J, Liang X, Jin MG, Xiao GQ, He JS, Pei YD. 2014. Geochemistry of clayey aquitard pore water as archive of paleo-environment, Western Bohai Bay. Journal of Earth Science, 26(3), 445–452. doi: 10.1007/s12583-014-0491-x.

Li J, Liang X, Zhang YN, Liu Y, Chen NJ, Abubakari A, Jin MG. 2017. Salinization of porewater in a multiple aquitard-aquifer system in Jiangsu coastal plain, China. Hydrogeology Journal, 25(8), 2377–2390. doi: 10.1007/s10040-017-1622-0.

Li X, Cui BS, Yang QC, Lan Y. 2016. Impacts of water level fluctuations on detritus accumulation in Lake Baiyangdian, China. Ecohydrology, 9(1), 52–67. doi: 10.1002/eco.1610.

Liu HY, Guo HM, Xing LN, ZhanYH, Li FL, Shao JL, Niu H, Liang X, Li CQ. 2016. Geochemical behaviors of rare earth elements in groundwater along a flow path in the North China Plain. Journal of Asian Earth Sciences, 117, 33–51. doi: 10.1016/j.jseaes.2015.11.021.

Liu HY, Guo HM, Yang LJ, Wu LH, Li FL, Li SY, Ni P, Liang X. 2015. Occurrence and formation of high fluoride groundwater in the Hengshui area of the North China Plain. Environmental Earth Sciences, 74(3), 2329–2340. doi: 10.1007/s12665-015-4225-x.

Ma Z, Xia YB, Li HT, Han B, Yu XZ, Zhou YL, Wang YS, Guo X, Li HQ, Pei YD. 2021. Analysis of natural resources and environment eco-geological conditions in the Xiong'an New Area. Geology in China, 48(3), 677–696 (in Chinese with English abstract). doi: 10.12029/gc20210301.

Niu H, Liang X, Lu GP, Peng F, Jin MG, Gu YS. 2017. A study of clay pore water and sporopollens for characterizing paleoenvironments in the Hebei Plain, Northern China. Journal of Asian Earth Sciences, 143, 1–10. doi: 10.1016/j.jseaes.2017.03.035.

Ortega-Guerrero A. 2003. Origin and geochemical evolution of groundwater in a closed-basin clayey aquitard, Northern Mexico. Journal of Hydrology, 284(1−4), 26–44. doi: 10.1016/S0022-1694(03)00239-7.

Pang ZH, Kong YL, Li J, Tian J. 2017. An isotopic geoindicator in the hydrological cycle. Procedia Earth and Planetary Science, 17, 534–537. doi: 10.1016/j.proeps.2016.12.135.

Qaisar M, Muhammad A, Muhammad R, Shanawar H, Waqas M, Muhammad AM, Muhammad I, Lubna A. 2020. Integration of geoelectric and hydrochemical approaches for delineation of groundwater potential zones in alluvial aquifer. Journal of Groundwater Science and Engineering, 8(4), 366–380. doi: 10.19637/j.cnki.2305-7068.2020.04.007.

Sacchi E, Michelot JL, Pitsch H, Lalieux P, Aranyossy JF. 2001. Extraction of water and solutes from argillaceous rocks for geochemical characterisation: Methods, processes, and current understanding. Hydrogeology Journal, 9(1), 17–33. doi: 10.1007/s100400000113.

Sadiq R, Husain T, Bose N, Veitch B. 2003. Distribution of heavy metals in sediment pore water due to offshore discharges: An ecological risk assessment. Environmental Modelling and Software, 18(5), 451–461. doi: 10.1016/S1364-8152(03)00010-0.

Shao JL, Li L, Cui YL, Zhang ZJ. 2013. Groundwater flow simulation and its application in groundwater resource evaluation in the North China Plain, China. Acta Geologica Sinica (English Edition), 87(1), 243–253. doi: 10.1111/1755-6724.12045.

Shi JS, Li GM, Liang X, Chen ZY, Shao JL, Song XF. 2014. Evolution mechanism and control of groundwater in the North China Plain. Acta Geoscientica Sinica, 35(5), 527–534 (in Chinese with English abstract). doi: 10.3975/cagsb.2014.05.01.

Song CQ, Ke LH, Pan H, Zhan SG, Liu K, Ma RH. 2018. Long-term surface water changes and driving cause in Xiong'an, China: From dense Landsat time series images and synthetic analysis. Science Bulletin, 63(11), 708–716. doi: 10.1016/j.scib.2018.05.002.

Sun YB, Wu SG, Dong DD, Lüdmann T, Gong YH. 2012. Gas hydrates associated with gas chimneys in fine-grained sediments of the northern South China Sea. Marine Geology, 311, 32–40. doi: 10.1016/j.margeo.2012.04.003.

Taheri M, Gharaie MHM, Mehrzad J, Afshari R, Datta S. 2017. Hydrogeochemical and isotopic evaluation of arsenic contaminated waters in an argillic alteration zone. Journal of Geochemical Exploration, 175, 1–10. doi: 10.1016/j.gexplo.2016.12.005.

Valle J, Gonsior M, Harir M, Enrich-Prast A, Schmitt-Kopplin P, Bastviken D, Conrad R, Hertkorn N. 2018. Extensive processing of sediment pore water dissolved organic matter during anoxic incubation as observed by high-field mass spectrometry (FTICR-MS). Water Research, 129, 252–263. doi: 10.1016/j.watres.2017.11.015.

Wang SQ, Song XF, Wang QX, Xiao GQ, Liu CM, Liu JR. 2009. Shallow groundwater dynamics in North China Plain. Journal of Geographical Sciences, 19(2), 175–188. doi: 10.1007/s11442-009-0175-0.

Xing LN, Guo HM, Zhan YH. 2013. Groundwater hydrochemical characteristics and processes along flow paths in the North China Plain. Journal of Asian Earth Sciences, 70–71, 250−264. doi: 10.1016/j.jseaes.2013.03.017.

Zhang YQ, Wang GW, Wang SQ, Yuan RQ, Tang CY, Song XF. 2018. Hydrochemical characteristics and geochemistry evolution of groundwater in the plain area of the Lake Baiyangdian watershed, North China. Journal of Groundwater Science and Engineering, 6(3), 220–233. doi: 10.19637/j.cnki.2305-7068.2018.03.007.

Zhang Z, Guo HM, Wang Z. 2018. Differences in major ions as well as hydrogen and oxygen isotopes of sediment pore water and lake water. Water Science and Engineering, 11(2), 147–156. doi: 10.1016/j.wse.2018.07.005.

Zhang ZH, Shi DH, Ren FH, Yin ZZ, Sun JC, Zhang CY. 1997. Evolution of Quaternary groundwater system in North China Plain. Science in China Series D: Earth Sciences, 40(3), 276–283. doi: 10.1007/BF02877536.

Zhu H, Yan BX, Pan XF, Yang YH, Wang LX. 2011. Geochemical characteristics of heavy metals in riparian sediment pore water of Songhua River, Northeast China. Chinese Geographical Science, 21(2), 195–203. doi: 10.1007/s11769-011-0448-2.

Zhu MJ, Wang SQ, Kong XL, Zheng WB, Feng WZ, Zhang XF, Yuan RQ, Song XF, Sprenger M. 2019. Interaction of surface water and groundwater influenced by groundwater over-extraction, waste water discharge and water transfer in Xiong'an New Area, China. Water, 11(3), 539. doi: 10.3390/w11030539.